

Weldability Evaluation of Supermartensitic Stainless Pipe Steels

A look at the as-welded mechanical properties of supermartensitic pipe steel welded joints, their susceptibility to hydrogen-induced stress corrosion, and the influence of short postweld heat treatment

BY J. E. RAMIREZ

ABSTRACT. Significant interest exists in the use of supermartensitic materials for oilfield applications. However, the hardness for both the weld deposit and the heat-affected zone (HAZ) of different material combinations may exceed the NACE requirement of 23 HRC (253 HV). Therefore, further studies to quantify the mechanical properties of welded joints and variables controlling the sulfide stress cracking (SSC) resistance in the as-welded condition remain necessary both for economical fabrication and to ensure reliable service operation. In this program, the as-welded mechanical properties of three different supermartensitic pipe steels were compared using different welding consumables and welding procedures. The susceptibility to hydrogen-induced stress corrosion cracking of selected weldments under slightly sour conditions and under cathodic protection was evaluated. Additionally, the influence of short postweld heat treatment (PWHT) on the HAZ mechanical properties and on the microstructure of three supermartensitic stainless pipe steels was studied. The results show that the filler metal and welding procedure combination affect the matching characteristics of the welded joint and their toughness and ductility properties. Additionally, supermartensitic steel welded joints with a maximum hardness ranging from 282 to 313 HV₁ and under an applied stress level equal to the measured yield strength of the base material did not crack under slightly sour conditions. The result also showed that a short PWHT is effective in reducing the microhardness of the HAZ to levels very close to the hardness of the base metal in the as-received condition. It is assumed that the main mechanism responsible for the changes of hardness with PWHT is the amount of reverted and stable austenite.

Introduction

Gradual depletion of easily obtainable hydrocarbons has accelerated the production of oil and gas from deep hot wells.

J. E. RAMIREZ (jose_ramirez@ewi.org) is with the Edison Welding Institute, Columbus, Ohio.

With the development of deep wells containing CO₂ and H₂S, many users began using corrosion-resistant alloys (CRAs). A variety of CRA materials are now commercially available in a range of tubular sizes. However, for reasons of cost, martensitic-type stainless steels are primarily used.

Supermartensitic stainless steels have been developed with higher resistance than conventional martensitic 13Cr to general and localized corrosion in CO₂ environments at elevated temperatures (Ref. 1). They are also sulfide stress cracking (SSC) resistant in environments containing a small amount of H₂S (Refs. 1, 2–6). In a typical supermartensitic stainless steel, the C content is reduced to below 0.03 mass percent in order to suppress the reduction of Cr concentration in the matrix due to Cr carbide precipitation, about 5.5 mass percent Ni content is added to obtain the martensite single phase, and 2 mass percent Mo content is added to improve SSC and localized corrosion resistance (Ref. 4). There are also supermartensitic steels that contain around 4% Ni and 1% Mo. Thus, supermartensitic steels can play an intermediate role between conventional martensitic 13Cr and duplex stainless steels regarding both the corrosion resistance and the material cost.

In general, supermartensitic stainless steels have good weldability. At carbon levels below 0.04% the hardness in the as-welded heat-affected zone (HAZ) of martensitic 13Cr base materials does not exceed 350 HV₁₀, which is considered to be the threshold of cold cracking. Therefore, a decrease in C content up to 0.03%

is effective to improve the resistance to cold cracking or hydrogen assisted cracking of the HAZ. Additionally, at this low carbon content, the microstructure changes from ferrite + martensite to simple martensite with the addition of Ni from 0 to 3%. Therefore, the high nickel content help limit the ferrite content or to completely avoid its occurrence in the HAZ and in the base material, which is the primary reason for any inadequate toughness or limited toughness in the HAZ of martensitic 13Cr steels.

The maximum hardness limit to avoid the potential for sulfide stress cracking in standard martensitic 13Cr steels, as well as for newer supermartensitic stainless steel, in CO₂/H₂S environments is 23 HRC per the NACE MR0175. However, reliable attainment of NACE MR0175 limits can be extremely difficult, particularly in weld metals (Ref. 7). Therefore, a postweld heat treatment (PWHT) operation probably cannot be avoided.

However, the PWHT is more complicated with supermartensitic steels. The presence of nickel depresses the A_{c1} temperature, so that tempering is necessarily carried out at fairly low temperatures, 600°–620°C. Tempering reactions therefore tend to be sluggish while, even with such a low temperature, the A_{c1} may be exceeded, leading to partial reformation of austenite during heat treatment and formation of virgin martensite on cool out. Maximum softening can normally be achieved using two stage heat treatment with a first intermediate cycle typically at 650–690°C and subsequent heat treatment at 600–620°C.

Therefore, it is desirable to obtain an estimate of the A_{c1} temperature to set PWHT conditions for different supermartensitic alloys. A fine balance must be struck between achieving a temperature high enough to give tempering, and low enough to restrict austenite formation, which will revert to virgin martensite on cooling. Some researchers (Ref. 8) pointed out that discernible hardening after a heat treatment occurs only when the A_{c1} is exceeded by a temperature interval sufficient to induce approximately 20% austenite. Unfortunately, a reliable

KEYWORDS

Supermartensitic Pipe Steels
Heat-Affected Zone (HAZ)
Sulfide Stress Cracking (SSC)
Postweld Heat Treatment (PWHT)
Welded Joints

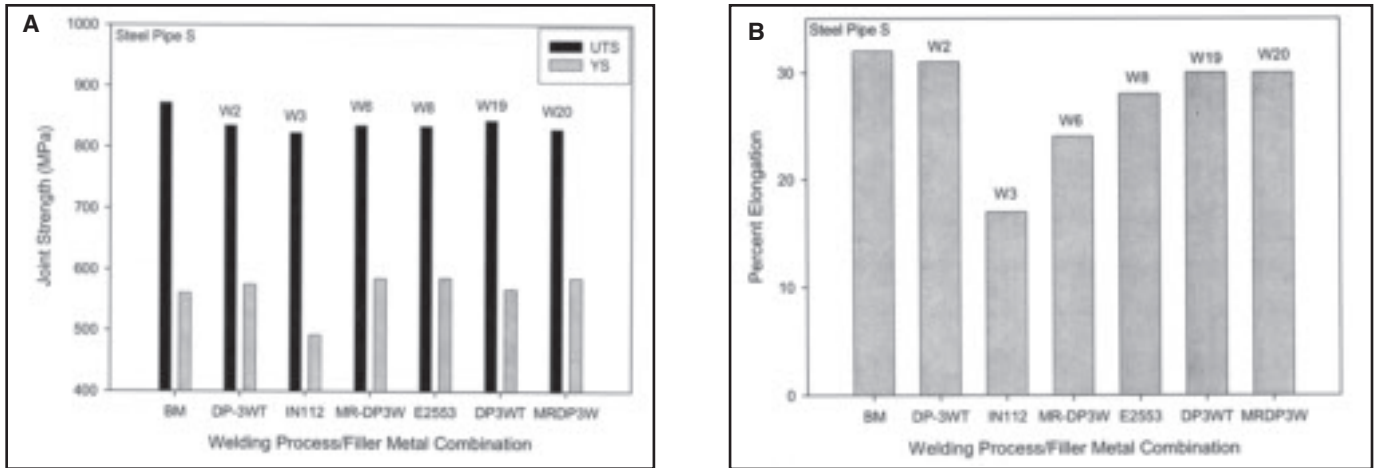


Fig. 1 — Tensile properties of supermartensitic steel pipe S welded joints. A — UTS and yield strength, and B — percent elongation.

Table 1 — Supermartensitic Pipe Steels, Welding Process, and Filler Metals

	S	K	N
Pipe inside diameter	228.6 mm (nominal)	5.2 in. (measured)	9.75 in. (measured)
Pipe wall thickness	12.3 mm (nominal)	0.3 in. (measured)	0.50 in. (measured)
	Pipe chemistry, wt-%		
	Reported	Analyzed	Analyzed
Carbon	0.007	0.031	0.013
Manganese	0.45	0.39	0.45
Phosphorus	0.018	0.012	0.017
Sulfur	0.0007	0.002	0.002
Silicon	0.31	0.16	0.16
Chromium	12.1	12.89	11.19
Nickel	6.2	3.96	6.24
Molybdenum	2.53	1.01	2.58
Titanium	0.07	Not measured	0.015
Copper	Not reported	Not measured	0.57
Nitrogen	0.004	Not measured	Not measured
	Filler Metals		
Welding Process			
SMAW	E2553, ENiCrMo-3 (IN112)	E2209, ENiCrMo-3 (IN112)	E2209, ENiCrMo-3 (IN112)
GMAW	MR-DP3W	—	—
GTAW	DP-3WT	—	—

relationship between composition and A_{c1} does not seem to have been produced for these alloys. Thus, further study of the transformation behavior of commercial supermartensitic steels in terms of both the A_{c1} and M_s/M_f temperatures, and of the tendency for supermartensitic steels to undergo re-austenization during tempering heat-treatment cycles is necessary.

On the other hand, in most situations, the sour environment will be present only on one side of the steel. In consequence, there will be a gradient of hydrogen concentration through the thickness, from high at the face in contact with the sour environment to very much lower at the free surface. The risk of cracking will therefore diminish through the thickness, so that higher hardnesses may be safely permitted on the outside of the pipe or pressure vessel. The relaxation possible has not been

fully defined, but, for wall thicknesses above some 10 mm, an external hardness of say 300 HV should be acceptable (Ref. 7).

Therefore, widespread application of supermartensitic steels depends upon solving the challenge of girth welding them in an economical way. At the same time, it should be recognized that blanket impositions of hardness or other limits can restrict welding procedures and increase fabrication costs. Further studies to quantify the mechanical properties of welded joints in the as-welded condition and variables controlling the SSC resistance remain necessary both for economical fabrication and to ensure reliable service operation. Short PWHT cycles are desirable for productivity reasons. However, recognizing the diffusional reactions involved in tempering, the effect of short PWHT on partial re-austenitization, degree

of softening, and the influence on toughness need to be evaluated for different supermartensitic steels.

In this study, the as-welded mechanical properties of three different supermartensitic pipe steels with a specified minimum yield strength of 80 ksi were compared using different welding consumables and welding procedures. The susceptibility to hydrogen-induced stress corrosion cracking of selected weldments under slightly sour conditions and under cathodic protection was evaluated. Additionally, the influence of short PWHT on mechanical properties and microstructure of Gleeble simulated HAZ of the three supermartensitic stainless pipe steels was also studied.

Experimental Procedures

Materials and Consumables: The general dimensions and chemical compositions of the three supermartensitic pipe steels, and the welding process/filler metal combinations that were used in this study are listed in Table 1. The three different pipe steels were identified as S, N, and K, respectively. In general, the supermartensitic steels S and N are of the type 13Cr-5Ni-2Mo and the steel K is of type 13Cr-4Ni-1Mo. Additionally, these three steels present some differences in the carbon content as indicated in Table 1. The filler metals DP-3WT and MR-DP3W (metal cored), and the covered electrode E2553 are designated as superduplex. The covered electrodes E2209 and ENiCrMo-3 (IN112) are duplex and nickel-based electrodes, respectively.

Welding: Welded sections of the three supermartensitic steel pipes were produced with the welding process and consumables combinations described in Table 2. Each section had a gas tungsten arc welding (GTAW) root pass made with DP-3WT wire. The rest of each joint was com-

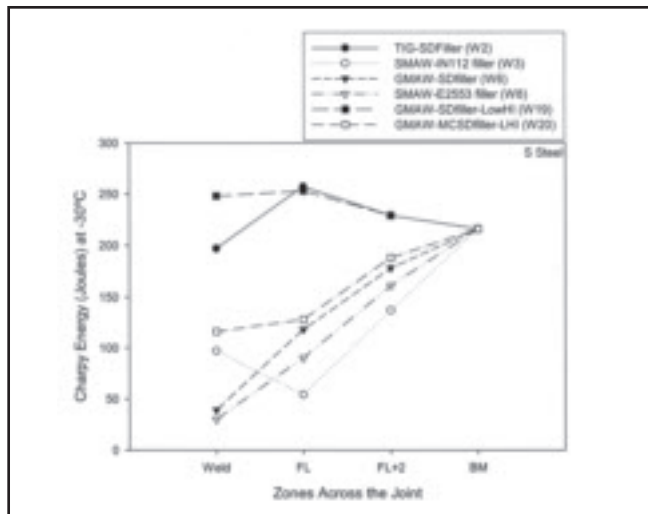


Fig. 2 — Charpy impact energy across welded joints of supermartensitic steel S as a function of welding process – filler metal combination.

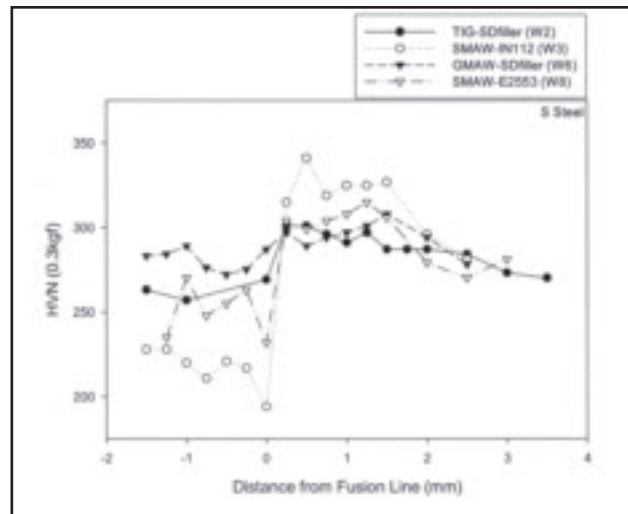


Fig. 3 — Microhardness profile near the cap of welded joints made with supermartensitic steel S.

pleted using GTAW, shielded metal arc welding (SMAW), or manual or mechanized gas metal arc welding (GMAW) process. No preheat was used and 150°C (300°F) maximum interpass temperature was maintained.

Mechanical Testing: The mechanical properties of the welded joints were characterized by using tensile and bend tests at room temperature. Charpy V-notch impact energy was determined at -30°C for the weld metal, fusion line, fusion line + 2 mm, and base metal locations. The weld metal, fusion line, and fusion line + 2 mm Charpy samples were taken near the 3, 6, and 12 o'clock positions of the weld. The weld metal, fusion line, and fusion line + 2 mm indicate the position of the middle of the sample relative to the welded joint.

Microstructural Characterization: Microhardness profiles were determined across some of the welded joints near the cap region. Additionally, the HAZ hardness of the joints W19 and W20 were determined at different through thickness locations. The microstructure of the fusion zone and HAZ of different welded joints were characterized using light microscopy after proper sample preparation.

Corrosion Testing: Selected supermartensitic welded joints and base metals were tested to evaluate their susceptibility to hydrogen-induced corrosion cracking under cathodic protection (CP) and under slightly sour (H₂S) service conditions. Table 3 shows a summary of the specimen identification, base material, loading method, specimen side in tension, and the type of corrosion tests that were carried out. The test conditions under CP and slightly sour environment are reported in Table 4. After testing specimens were cut, mounted, and polished. Visual inspection with a magnification of up to 1000× was

performed on all tested specimens to observe any cracks.

Influence of Short PWHT on Gleeble Simulated HAZ:

The transformation temperatures, A_{C1} and martensite start formation, for each one of the steels were determined by dilatometric analysis. Heat-affected zone weld simulations were performed with a peak temperature of roughly 1350°C and a cooling rate between 800° and 500°C of 40°C/s simulating normal GMAW heat inputs. A PWHT was performed in a Gleeble machine, at temperatures equal to A_{C1} , $A_{C1} + 40°C$, and $A_{C1} - 40°C$, for 5 and 10 min. The resulting HAZ mechanical properties (hardness and impact Charpy V-notch energy) and microstructure of three supermartensitic stainless pipe steels were evaluated.

Results and Discussions

Tensile Properties: The observed tensile properties of the supermartensitic welded joints are listed in Table 5 and some of the results are shown in Fig. 1. The welded joint made with ENiCrMo-3 (IN112) or duplex filler metal failed in the weld metal. Welded joints made with superduplex filler metal failed in the base metal. The yield strength of all the joints welded with either duplex or superduplex filler metal was higher than 550 MPa (80

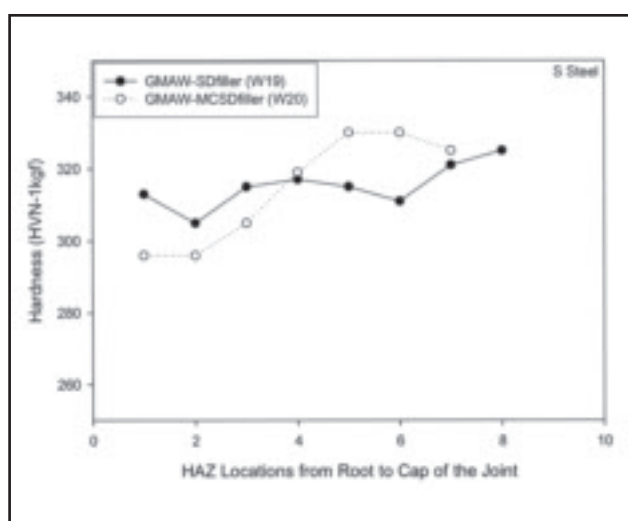


Fig. 4 — Microhardness of HAZs at different through-thickness locations of welded joints made with supermartensitic steel S.

ksi). The percent elongation measured in the tensile test samples of the supermartensitic steel welded joints ranged from about 6 to 33.

Normally, oil and gas companies require a yield strength overmatching in the weld metal of circumferential joints in comparison with the pipe material. Therefore, Ni-base electrodes (ENiCrMo-3) are not recommended to join X80 grade supermartensitic steel pipes due to the resulting undermatching condition of the weld metal. The duplex and superduplex consumables provided an increasing degree of overmatching in the weld metal of X80 supermartensitic steel pipe joints.

The range of 6 to 33% elongation observed in the supermartensitic steel joints is influenced by the welding consumable, matching characteristics of the joints, and

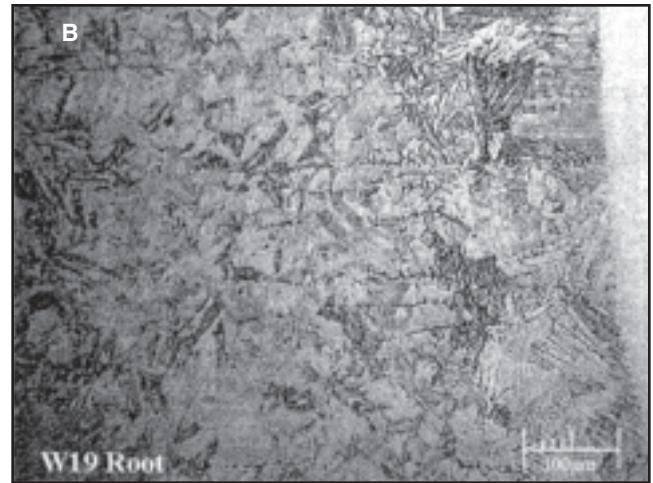
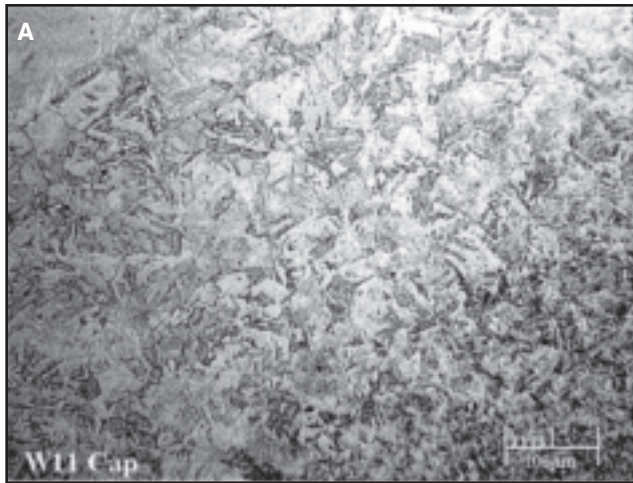


Fig. 5 — Microstructures observed in the intermixing zone of the weld metals and in the HAZs of the supermartensitic steels. A — Cap; B — root.

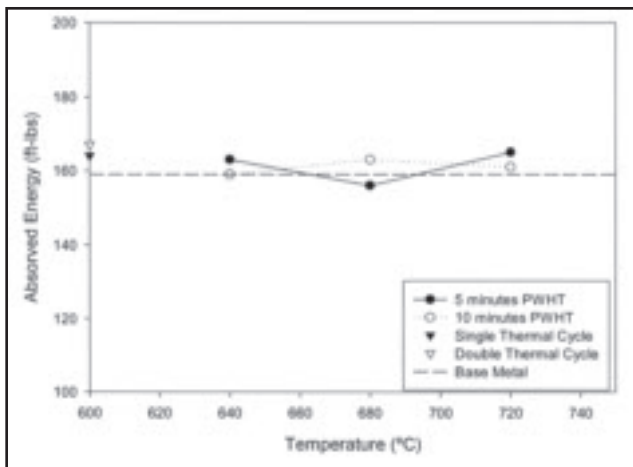


Fig. 6 — Charpy V-notch absorbed energy at -30°C in simulated HAZ from supermartensitic pipe steel S as a function of thermal experience.

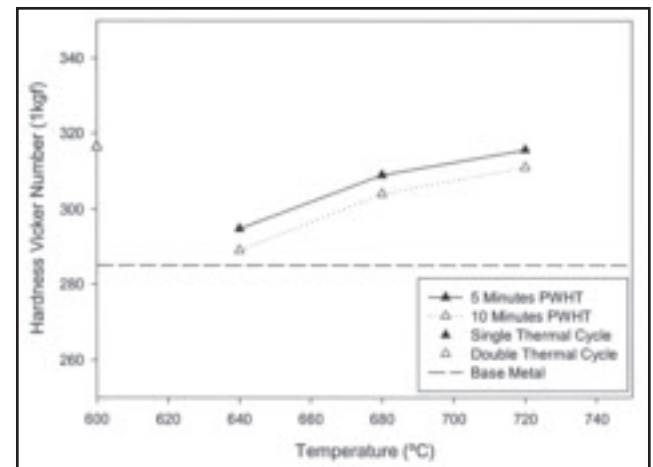


Fig. 7 — Hardness of simulated HAZ from pipe steel S as a function of thermal experience.

welding procedure used. Joints made with duplex and superduplex consumables using SMAW, GMAW, and GTAW processes show an elongation between 20 to 33%. The lower levels of ductility (14–15% elongation) measured in the joints made with the nickel-base electrode (ENiCrMo-3) may be explained by the concentration of plastic deformation in the weld during the tensile test as a result of the undermatching characteristics of the weld metal. Most of the plastic deformation is localized in the weld metal instead than in the complete gauge length. However, the lowest level of ductility (6% elongation) in the welded joints was observed in a K steel joint made with the nickel-base electrode without heat input control using a weave technique. The further decrease in ductility may have resulted from the formation of niobium ni-

tride due to migration of nitrogen from the base metal into the niobium-rich weld metal. K steel has the highest reported level of nitrogen out of the three supermartensitic steels used in this study as shown in Table 1.

Impact Absorbed Energy: It was observed, in general, that the absorbed energy in the welded joints at -30°C decreased from the base metal to the fusion line and to the weld metal. The average impact energy of the supermartensitic steel pipes was about 200 joules. The decrease in impact energy in the fusion line and HAZ of the supermartensitic welded joints as compared to the base metals is considered to be a result of the microstructural variation present near the fusion lines in these dissimilar metal joints. The microstructural variation is a result of the inevitable compositional gra-

dient across the fusion boundary of these welding joints with nonmatching consumables. Additionally, the untempered condition of the martensite and the present of strings of ferrite in the HAZ, as discussed in the following section, may have also affected the absorbed impact energy.

The impact energy of the weld metal depends on the welding procedures and filler metals used for welding the pipe joints. Increasing average weld metal impact energies in the range between 30 to 248 joules are achieved with the SMAW, GMAW, GMAW with heat input control, and GTAW process, respectively. Decreasing impact energies are obtained in nickel-base, duplex, and superduplex weld metals deposited without heat input control. The minimum impact energy of the welded joints ranged from 25 to 181 joules. The Charpy V-notch impact testing

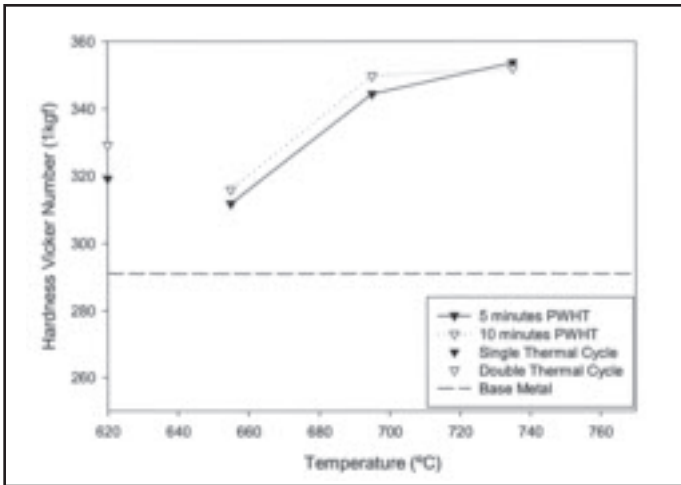


Fig. 8 — Hardness of simulated HAZ from pipe steel N as a function of thermal experience.

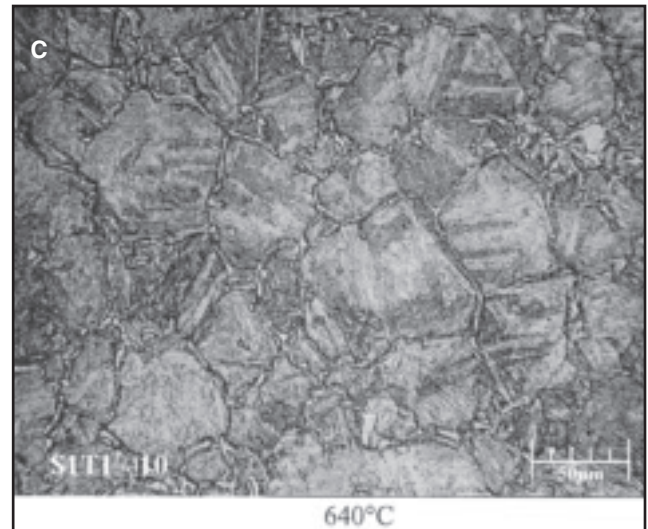
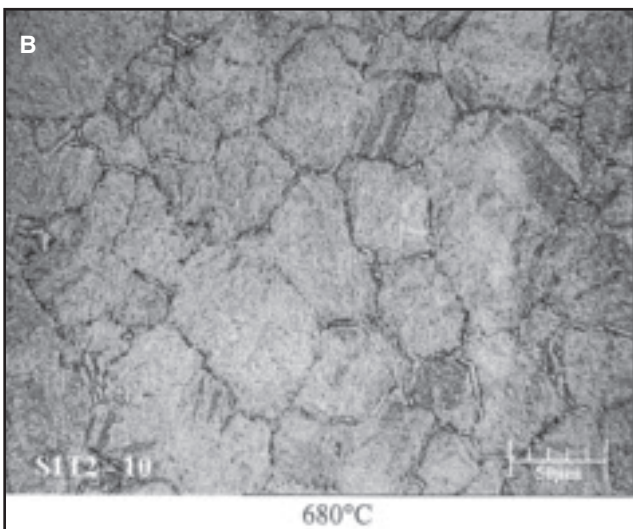
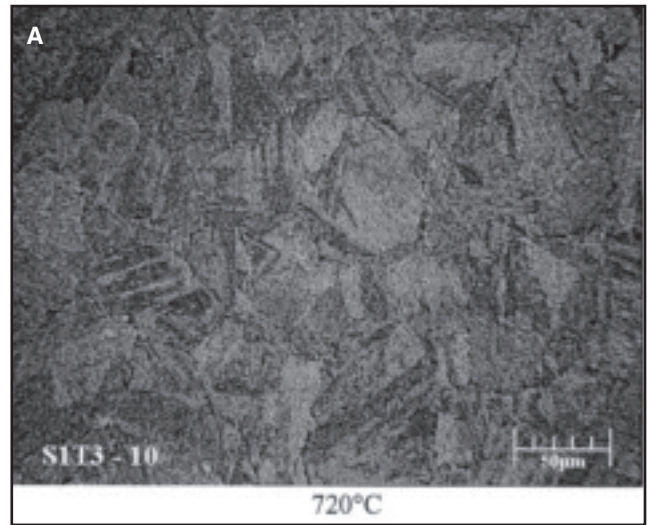


Fig. 9 — Fraction of retained austenite at room temperature in a simulated HAZ from pipe steel S after PWHT for 10 min at different temperatures. A — 720°C; B — 680°C; C — 640°C.

results of supermartensitic pipe steel S is shown in Fig. 2.

The increasing weld metal impact energies achieved with the SMAW, GMAW using a weave technique, GMAW with heat input control, and GTAW process can be explained based on two main factors. First, a higher level of inclusions in the weld metal is expected in joints made with a flux-shielded process such as SMAW as compared to joints made with gas-shielded processes such as GMAW and GTAW. The higher the level of inclusions in the weld metal, the lower the expected impact absorbed energy. Second, duplex and superduplex weld metals are very susceptible to the formation of intermetallic compounds that affect the impact absorbed-energy of the weld metal. A high heat input or weave technique decreases

the cooling rate and, therefore, increases the susceptibility to the formation of intermetallic compounds. This results in decreasing impact energies in welds made with nickel-base (ENiCrMo-3), duplex, and superduplex consumables and deposited without heat input control. Therefore, the weld metals with the best impact absorbed energies are obtained with gas-shielded processes such as GMAW and GTAW, and with control of heat input to avoid the formation of intermetallic compounds in the duplex and superduplex microstructures.

However, most of the welding process-filler metal combinations used to weld the different supermartensitic steel pipes are expected to provide average impact energies in the welded joints above the minimum absorbed energy of 27 to 40 joules at

–30°C required for different industrial applications.

Microstructural Characterization: The maximum hardness of the HAZ corresponding to different base metal/filler metal/welding process combinations is listed in Table 6. The maximum hardness of the HAZs near to the cap region range from 301 to 341, 346 to 362, and 378 to 391 HV₁ in the supermartensitic steels S, N, and K, respectively. The hardness of the three supermartensitic steels ranges from 281 to 301 HV₁ and is included in Table 6 as a reference. Figure 3 shows the microhardness profiles across different welded joints corresponding to different filler metal/welding process combinations used to weld supermartensitic pipe steel S. Figure 4 shows the hardness of the HAZs in different through-thickness locations of

Table 2 — Characteristics of Different Welded Pipe Sections

Weld ID	Base Metal	Welding Process	Filler Metal ^(a)	Shielding Gas
W1	S	Manual GTAW	1.2-mm DP-3WT	Argon
W2		Manual GTAW	1.2-mm DP-3WT	Argon
W3		SMAW	3/32-in. ENiCrMo-3	None
W4		SMAW	3/32-in. ENiCrMo-3	None
W5		SMAW	3/32-in. ENiCrMo-3	None
W6		GMAW	1.2-mm MR-DP3W	Argon
W7		GMAW	1.2-mm MR-DP3W	Argon
W8		SMAW	3/32-in. E2553	None
W9		SMAW	3/32-in. E2553	None
W19			Mech. GMAW	1.2-mm DP-3WT
W20		Mech. GMAW	1.2-mm MR-DP3W	Argon
W10	N	SMAW	3/32-in. ENiCrMo-3	None
W11		SMAW	3/32-in. E2209	None
W12		SMAW	None (only root pass)	None
W13	K	SMAW	3/32-in. ENiCrMo-3	None
W14		SMAW	3/32-in. ENiCrMo-3	None
W15		SMAW	3/32-in. ENiCrMo-3	None
W16		SMAW	3/32-in. E2209	None
W17		SMAW	3/32-in. E2209	None

(a) One to three root passes were deposited in each weld with GTAW using 1.2-mm DP-3WT wire.

Table 3 — Summary of Cathodic Protection and Slightly Sour Condition Testing

Sample	Material	Maximum Hardness, HV ₁	Loading Method	Side in Tension	Test
W2	S	301	4-point Bend	Cap	CP
W19	S	320	4-point Bend	Cap	CP
W20	S	320	4-point Bend	Cap	CP
W8	S	315	4-point Bend	Cap	CP
W11	N	346	4-point Bend	Cap	CP
W17	K	378	4-point Bend	Cap	CP
W2	S	301	4-point Bend	Root	H ₂ S
W19	S	313	4-point Bend	Root	H ₂ S
W20	S	296	4-point Bend	Root	H ₂ S
W2	S	301	3-point Bend	Root	H ₂ S
W19	S	313	3-point Bend	Root	H ₂ S
W20	S	296	3-point Bend	Root	H ₂ S
Base Metal	S	282	3-point Bend	Base metal	H ₂ S

two welded joints. The hardness of the HAZ shows an increasing trend from the root to the cap region of the joint.

The microstructure of the weld metals ranges from fully austenitic in welds made with the Ni-base (ENiCrMo-3) electrode to a ferritic-austenitic duplex microstructure with different levels of ferrite and austenite in welds made with the duplex and superduplex filler metals. The microstructure observed in the HAZ of the supermartensitic steel pipes corresponds to untempered martensite as shown in Fig. 5. Figure 5B shows some strings of retained ferrite observed in the coarse-grained HAZ of the supermartensitic steel S. In the intermixing zone of the weld metal near to the fusion line, a variety of microstructures were present.

The increasing maximum hardness

Table 4 — Test Conditions under CP and Slightly Sour Environments

Parameter	Test		
	Cathodic Protection	Slightly Sour Environment	
Solution	NACE-seawater	Procedure A NACE-seawater	Procedure B 5%NaCl + Water + Buffer solution ^(a)
pH	8.2	3.5–4.0	3.0–3.5
CO ₂ Pressure	None	3 MPa (435 lb/in. ²)	3 MPa (435 lb/in. ²)
H ₂ S Pressure	None	0.001 MPa (0.15 lb/in. ²)	0.001 MPa (0.15 lb/in. ²)
Polarization (SCE)	–800 mV	Free corrosion potential	Free corrosion potential
Applied Stress	100% yield strength of base metal	100% yield strength of base metal	100% yield strength of base metal
Loading Mode	Four-point bending	Four-point bending	Three-point bending
Specimen Geometry (in.)	Flat-bar specimens 5.5 × 0.675 × 0.275	Flat-bar specimens 5.5 × 0.675 × 0.275	Flat-bar specimens 1.7 × 0.675 × 0.125
Temperature, °C	25 ± 2	25 ± 2	25 ± 2
Exposure Time	30 days	30 days	30 days

(a) Solution containing CH₃COONa-CH₃COOH to control pH.

ranges of 301 to 341, 346 to 362, and 378 to 391 HV₁ observed in the HAZs near to the cap in the supermartensitic steel S, N, and K welded joints are in agreement with the expected trend in untempered martensite microstructures with increasing levels of carbon. The carbon content in the steel controls the hardness level in the untempered martensitic microstructure. As reported in Table 1, the carbon content in S, N, and K steels is 0.007, 0.013, and 0.031, respectively. The tempering effect of subsequent passes induces some softening of the HAZ in the root and results in the increasing hardness levels observed in the through-thickness microhardness profile from the root to the cap zone in the welded joints.

The hardness for the welding deposits and the HAZ of all the material-welding process-welding consumables combinations tested in this program exceeds the NACE requirements of 23 HRC (253 HV). Additionally, the hardness of the as-received supermartensitic steel pipes ranges from 282 to 301 HV₁, therefore, is also above the maximum hardness limitations established by NACE.

However, there are several issues that need to be addressed regarding the maximum hardness of 23 HRC allowed by NACE for use of supermartensitic steels in sour service. First, it has been indicated that the ASTM E140 and BS 860: Rockwell-Vickers correlations are not applicable to 13Cr-4Ni steels (Ref. 8), and if the Hays-Patrick relationship is accepted, the NACE limit of 23 HRC can be taken as equivalent to 275 H_V instead of 253 (Ref. 8). Second, in most situations the sour environment will be present only on one side of the steel. Consequently, there will be a gradient of hydrogen concentration through the thickness, from high at the face in contact with the sour environment to very much lower at the free surface. The risk of cracking will therefore diminish through the thickness, so that higher hardness may be safely permitted on the outside of the pipe. The amount of hardness relaxation in supermartensitic steels has not been fully defined. For example, in C-Mn steels with a wall thickness above 10 mm, an external hardness maximum has been relaxed from 248 to 300 HV (Ref. 7). Additionally, the softening of the HAZ in the root region of the welded joint induced by the tempering effect of subsequent passes will reduce the susceptibility to SSC in supermartensitic steel welded joints. Third, there is a need to document maximum hardness levels in supermartensitic steel for sour service, as the existing criteria are lower than the hardness of the pipe materials as delivered.

Hydrogen-Induced Corrosion Cracking under CP or Slightly Sour Conditions:

Table 5 — Tensile Test Results

Sample ID Area	Tensile Strength	Yield Strength	Elongation	Reduction	Fracture
	MPa (ksi)	MPa (ksi)	(%)	in Area (%)	
Steel Pipe S					
BM-T1	872 (126.5)	565 (82.0)	31.7	72.1	—
BM-T2	871 (126.3)	557 (80.8)	31.6	72.2	—
W2-T1	834 (121.0)	565 (81.9)	31.1	71.6	Base
W2-T2	836 (121.3)	586 (85.0)	30.5	71.0	Base
W3-T1	834 (120.9)	488 (70.8)	14.9	28.5	Weld
W3-T2	812 (117.7)	496 (71.9)	18.4	32.6	Weld/HAZ
W6-T1	842 (122.1)	579 (84.0)	25.8	71.4	Base
W6-T2	829 (120.2)	592 (85.9)	21.2	74.3	Base
W8-T1	841 (121.9)	586 (85.0)	27.8	66.7	Base
W8-T2	827 (120.0)	587 (85.2)	28.6	72.6	Base
W19-T1	838 (121.5)	564 (81.8)	29.4	70.3	Base
W19-T2	848 (123.0)	570 (82.7)	31.5	70.2	Base
W20-T1	834 (121.0)	574 (83.2)	32.3	67.1	Base
W20-T2	823 (119.4)	598 (86.7)	27.5	72.4	Base
Steel Pipe N					
BM-T1	866 (125.6)	652 (94.5)	19.9	59.6	—
BM-T2	866 (125.6)	675 (97.9)	23.4	63.2	—
W10-T1	834 (121.0)	491 (71.2)	13.8	34.0	Weld
W10-T2	821 (119.0)	523 (75.8)	14.5	56.7	Weld
W11-T1	839 (121.7)	604 (87.6)	20.0	43.8	Weld
W11-T2	838 (121.5)	579 (84.0)	20.2	42.6	Weld
Steel Pipe K					
BM-T1	849 (123.2)	698 (101.2)	23.9	70.7	—
BM-T2	847 (122.9)	703 (101.9)	23.7	69.5	—
W14-T1	754 (109.4)	537 (77.9)	5.7	23.0	Weld
W14-T2	777 (112.7)	561 (81.4)	6.4	21.3	Weld
W16-T1	824 (119.5)	623 (90.3)	18.8	72.5	Weld
W16-T2	845 (122.6)	627 (91.0)	21.3	71.9	Weld

Table 6 — Maximum HAZ Hardness Near the Cap Region of the Welded Joints

Base Metal	Welding Process-Filler Metal	Maximum HAZ Hardness, HV ₁
S	Base Metal	282
	GTAW-SD filler	301
	SMAW-ENiCrMo-3	341
	SMAW-E2553	315
	GMAW-SD filler	308
N	Base Metal	301
	SMAW-ENiCrMo-3	362
	SMAW-E2209	346
K	Base Metal	282
	SMAW-ENiCrMo-3	391
	SMAW-E2209	378

Table 7 lists a summary of the results of the testing under CP and under slightly sour conditions. Even though the applied stresses used in this experimental work were equal to the measured yield strength of the base metals, and the maximum hardness of different specimens tested under cathodic protection (–800 mV SCE) or under slightly sour conditions (0.001 MPa, 0.15 lb/in.² P_{H2S}) ranges from 301 to 378, and from 282 to 313 HV₁, respectively, cracking was not observed.

These results indicate that under the testing conditions used, the tested supermartensitic steels are not susceptible to cracking under either proper CP or under

slightly sour conditions at hardness level above the 23 HRC (253 HV) limit established by NACE.

The observed resistance to SSC in slightly sour conditions of the tested supermartensitic steels in spite of the high level of hardness may be explained based on the good corrosion resistance of these materials that results in low corrosion rates. The SSC behavior of typical martensitic stainless steel has been explained based on the decrease of the hydrogen diffusion coefficient with an increase in content of alloying elements. Since hydrogen content in steel is proportional to the inverse of the hydrogen diffusion coefficient

Table 7 — Summary of Test Results (Cracking) for Corrosion Testing under CP and Sour Conditions

Specimen	Steel	Test	Hardness, HV ₁	Results
W2	S	CP-Cap tension	301	No cracking
W19	S	CP-Cap tension	320	No cracking
W20	S	CP-Cap tension	320	No cracking
W8	S	CP-Cap tension	315	No cracking
W11	N	CP-Cap tension	346	No cracking
W17	K	CP-Cap tension	378	No cracking
W2	S	H ₂ S-Root Tension-Procedure A	282–301	No cracking
W19	S	H ₂ S-Root Tension-Procedure A	313	No cracking
W20	S	H ₂ S-Root Tension-Procedure A	296	No cracking
W2	S	H ₂ S-Root Tension-Procedure B	282–301	No cracking
W19	S	H ₂ S-Root Tension-Procedure B	313	No cracking
W20	S	H ₂ S-Root Tension-Procedure B	296	No cracking
Base metal	S	H ₂ S-BM Tension-Procedure B	282	No cracking

Table 8 — Transformation Temperatures of Supermartensitic Pipe Steels S, N, and K

Pipe Steel	A _{c1} (°C)	A _{c1} ^(a)	A _{c3} (°C)	Ms (°C)
S	680	630	780	201
N	695	602	765	224
K	745	680	820	277

(a) Determined based on chemical composition.

$$A_{c1} (\text{°C}) = 850 - 1500(C + N) - 50Ni - 25Mn + 25Si + 25Mo + 20(Cr-10) \text{ (Ref. 9)}$$

cient, the hydrogen content in high-chromium steel may become quite large. As result, the high-Cr steel may have a high susceptibility to hydrogen embrittlement due to the smaller hydrogen diffusion coefficient. Therefore, the best way to control the susceptibility to hydrogen embrittlement of high-Cr steels is by decreasing the hydrogen permeation rates. The low corrosion rate of supermartensitic steel decreases the amount of hydrogen generated on the surface, which may result in lower hydrogen permeation rates in the steel a better SCC resistance.

Materials may also be susceptible to hydrogen embrittlement caused by cathodic protection dependent on the environmental conditions. The lower limit of the cathodic protection is in principle limited by the hydrogen equilibrium potential. The hydrogen evolution potential is a function of the pH and is equal to $(-0.24-0.059 \text{ pH}) V_{SCE}$. For a pH of 8.2, the hydrogen evolution potential is equal to $-0.72 V_{SCE}$. Therefore, the potential of $-0.8 V_{SCE}$ impressed on the sample during the CP testing was more negative than the hydrogen evolution potential and demonstrates the hydrogen-induced cracking resistance observed in the tested supermartensitic steels.

Therefore, supermartensitic 13Cr steel can be perfectly protected against corrosion without any risk of hydrogen embrittlement when the cathodic protection is

properly controlled between the protection potential and the hydrogen evolution potential. In practice, the production of hydrogen is expected to be very limited at a potential slightly lower than the hydrogen equilibrium potential and, in the absence of H₂S, potentials 100 mV lower than the hydrogen equilibrium potential may be acceptable in practice.

Influence of Short PWHT on Gleeble Simulated HAZ: The transformation temperatures of pipe steels S, N, and K, as determined by dilatometer analysis, are shown in Table 8. Additionally, the temperature at which the austenite starts to form during heating, A_{c1}, was determined based on chemical composition, and it is also included in Table 8 as a comparison. The A_{c1} temperature, based on chemical composition, was determined using an equation that was developed empirically from data for 13Cr steels with carbon content below about 0.05 wt-% (Ref. 9). The difference between the transformation temperatures of the different supermartensitic pipe steels can be explained based on the effect of the alloying elements, especially Ni, on the stability of austenite.

The impact Charpy V-notch toughness of the HAZs of pipes S and N in every thermal condition, single-/double-thermal cycle, and tempered at temperatures equal to A_{c1}, A_{c1} + 40°C, and A_{c1} - 40°C, for 5 and 10 min, were equal, or higher

than the toughness of the base metal in the as-received conditions. The results of the Charpy V-notch tests for the HAZ of supermartensitic pipe steel S is shown in Fig. 6. On the other hand, the toughness of the simulated HAZ of pipe steel K after a single- and double-thermal cycle, and after PWHT at 785°C was lower than the base metal in the as-received condition. However, metallographic evaluation of samples from the simulated HAZ of pipe K material indicated a nonuniform microstructure as the result of a nonuniform thermal experience across the section of the sample. This may have resulted from an improper contact between the samples and the grips in the Gleeble machine. Due to the size of the pipe, specimens from pipe steel K were subsized. Therefore, the results obtained from the evaluation of the simulated HAZ from pipe steel K are considered to be invalid, and no further analysis was attempted from the samples prepared from pipe steel K.

The microhardness of the simulated HAZs of supermartensitic pipe steels S and N after different welding thermal cycles and PWH treatments are listed in Table 9. Figures 7 and 8 show how the average microhardness of the simulated HAZs of pipe steels S and N changed with thermal cycles and with temperature and holding time during tempering. The microhardness of the HAZs from pipe S increases from 285 to 316 HVN (1 kgf) after a single- or double-thermal cycle. Tempering at 720°C does not affect the hardness of the HAZ. However, as the tempering temperature decreases from 720° to 640°C, the microhardness decreases. A microhardness of 289 HVN is obtained in the HAZ after a PWHT at 640°C for 10 min — Fig. 7. This result shows that a short PWHT is effective to reduce the microhardness of the HAZ to levels very close to the hardness of the base metal in the as-received condition. As shown in Fig. 8, single- and double-thermal cycles increase the hardness of the HAZ of pipe steel N from 291 to 320 and 330 HVN, respectively. Postweld heat treatment of the HAZ at 735° and 695°C for 5 and 10 min further increases the hardness to about 350 HVN. However, PWHT at 655°C for 5 and 10 min softens the HAZ to a level of about 314 HVN.

A fully martensitic microstructure was observed in the simulated HAZ of both pipes steel S and N after a single-thermal cycle. The main characteristic observed in pipe steel S was the increase of retained austenite, at the grain boundaries, as the tempering temperature was decreased from 720° to 640°C as shown in Fig. 9. The fraction of retained austenite in the grain boundaries increases with holding time during PWHT. On the other hand, etching

Table 9 — Results of Hardness Measurements [HVN (1 kgf)] in Simulated HAZ from Pipe Steels S and N after Different Thermal Cycles and PWHT

Specimen	HVN (1 kgf)	Average HVN	Specimen	HVN (1 kgf)	Average HVN
Base Metal		285	Base Metal		291
S1	318 319.5 315.5 313	316.5	N1	318 315 318 326	319.2
S2	315.5 321 314.5 317.5 313	316.3	N2	326 329 326 338 327	329.2
S1T3-5	314 311 319.5 318	315.6	N1T3-5	350 356 354 355	353.7
S1T3-10	319 309.5 316.5 299.5	311	N1T3-10	335 340 357 357 355 351	352
S1T2-5	305 303 306 316 315	309	N1T2-5	345 346 345 314 340 346	344.4
S1T2-10	300 310.5 298.5 307	304	N1T2-10	350 354 350 345	349.8
S1T1-5	302 293 291 293	294.8	N1T1-5	306 314 318 309	311.8
S1T1-10	279 295 291 291	289	N1T1-10	309 316 318 321	316

of pipe steel N only revealed very small amounts of retained austenite at the grain boundaries when PWH treated at 695°C.

The increasing fraction of austenite observed in pipe steel S as the PWHT temperature is decreased from 720° to 640°C is the result of the reversion and stability of austenite as a function of time and temperature. At PWHT temperature, reformation of austenite is promoted. Since the reaction is diffusion controlled, the austenite formed after PWHT will differ compositionally from austenite retained after the welding operation. In the latter case, the martensitic matrix and residual austenite will be of identical composition, whereas the reverted austenite formed during heat treatment will be enriched in Ni, C, and N. The degree of enrichment determines the stability of the austenite formed during the PWHT operation. If the A_{c1} is exceeded only slightly, by say 40°C, then the enriched austenite formed will be stable on cooling to room temperature. At temperatures further above the A_{c1} point, the equilibrium austenite con-

tent is greatly increased, the relative enrichment is reduced, and on cooling to room-temperature transformation to virgin martensite will occur, thus decreasing the amount of austenite retained at room temperature.

Based on the microstructural analysis and as expected, the A_{c1} determined by dilatometry is higher than the equilibrium-transformation temperature. The heating rate affects the transformation temperature determined by dilatometry; the higher the heating rate, the higher the transformation temperature. According to the microstructural analysis, the equilibrium-transformation temperature for pipe steel S is below 640°C.

To some degree, the effect of PWHT depends on the M_f of the alloy. If this is low, substantial austenite will be retained at room temperature after PWHT simply because the material remains above the M_f point. However, PWHT may induce sufficient carbide precipitation to deplete the matrix of C and raise the Ms. The austenite is destabilized and will trans-

form to virgin martensite on cooling from the PWHT temperature; the reaction sequence depends on the C content of the steel, and the effect will be of less significance with very-low-C alloys. The resulting higher Ms temperature of pipe steel N may be responsible for the absence of any major fraction of austenite at room temperature.

An important additional consideration is the effect of retained austenite on the corrosion performance of supermartensitic stainless steel pipe. It has been observed that there is no harmful influence of retained austenite on the corrosion resistance of supermartensitic steels (Ref. 10). Additionally, a higher content of retained austenite reduces the diffusible hydrogen and the SSC susceptibility of the steel. Due to the high solubility of hydrogen in austenite, austenite act as a hydrogen trap and reduces the effective diffusion coefficient of hydrogen.

The changes in the mechanical properties on tempering can now be discussed on the basis of the microstructural changes. It

is assumed that three mechanisms are responsible for the changes of hardness with PWHT, i.e., reversion of austenite, reduction in dislocation density, and precipitation. In pipe steel S, the hardness decreases with a decrease in PWHT temperature from 720° to 640°C and an increase in holding time from 5 to 10 min due to the increase in the fraction of stable austenite. Additionally, a reduction in dislocation density and decrease of C level in the untransformed martensite may also influence the hardness level. On the other hand, the hardness of pipe steel N increases with PWHT at the two highest temperatures, 735° and 695°C. Higher levels of C and lower levels of Ti in pipe steel N as compared to pipe steel S may increase the susceptibility to secondary hardening during PWHT due to the formation of carbides based on V, Cr, or Mo. Additionally, the formation of Cu precipitates may also play a factor in the increase of hardness during PWHT at the two highest temperatures. Softening of the HAZ of pipe steel N during PWHT at 655°C may result from a reduction dislocation density and from the fact that some C has been taken out of solid solution and has formed some carbides.

Conclusions

The following conclusions can be drawn from this work:

- Nickel-base ENiCrMo-3 electrodes are not recommended to join X80 grade supermartensitic steel pipes due to the resulting undermatching condition of the weld metal and the low levels of ductility (6 to 15% elongation) of the welded joints.
- Duplex and superduplex consumables provided an increasing degree of overmatching in the weld metal of X80 supermartensitic steel pipe joints resulting in a yield strength of the joint above 550 MPa (80 ksi) and an elongation between 20 to 33% when using SMAW, GMAW, and GTAW processes.
- All of the welding process-filler metal combinations used to weld the different supermartensitic steel pipes provided averaged impact energies in the welded joints above the minimum absorbed energy of 27 to 40 joules at -30°C required for different industrial applications.
- The maximum hardness observed in the HAZ near to the cap in the S, N, and K supermartensitic steel welded joints ranges from 301 to 341, 346 to 362, and 378 to 391 HV₁, respectively. The hard-

ness of the weld metal and HAZ resulting from all the material-welding process-welding consumables combinations exceeds the NACE requirements of 23 HRC (253 HV).

- The tested supermartensitic steels are not susceptible to cracking under either CP or slightly sour conditions at hardness levels above the 23 HRC (253 HV) limit established by NACE, under the testing conditions used including an applied stress level equal to the measured yield strength of the base material.
- The transformation temperature at which the austenite starts to form during heating, A_{c1}, of pipes steels S, N, and K, as determined by dilatometric analysis, are 680, 695, and 745°C, respectively. The martensitic start temperatures, M_s, are 201°, 224°, and 277°C for pipes S, N, and K steel, respectively. According to the microstructural analysis, the equilibrium-transformation temperature, A_{c1}, for pipe steel S is below 640°C.
- The fraction of retained austenite in the simulated HAZ in pipe steel S at room temperature increases as the tempering temperature was decreased from 720° to 640°C and increases with hold time during PWHT.
- A microhardness of 289 HVN is obtained in the HAZ of supermartensitic pipe steel S after a PWHT at 640°C for 10 min. This result shows that short PWHT are effective for reducing the microhardness of the HAZ to levels very close to the hardness of the base metal in the as-received condition.
- The toughness of the simulated HAZ of pipe steels S and N in every thermal condition, single-/double-thermal cycle, and after PWHT is equal to or higher than the toughness of the base metal in the as-received conditions. In general, the change in toughness reflected the change in hardness; i.e., a reduction in hardness was accompanied by an increase in toughness.

References

1. Duisberg, J., Niederhoff, K. A., and Popperling, R. K. 1996. 13%Cr steels for flow-line and pipeline applications. *Stainless Steel World* 8(6): 29-33.
2. Biagiotti, Jr., S. F., and Reichman, J. S. 1995. Justifying the use of 13Cr for corrosive CO₂ operations. *Corrosion/95*, Paper 81, NACE International, Houston, Tex.
3. Ueda, M., Amaya, H., Kondo, K., Ogawa, K., and Mori, T. 1996. Corrosion resistance of weldable super 13%Cr stainless steel in H₂S

containing CO₂ environments. *Corrosion/96*, Paper 58, NACE International, Houston, Tex.

4. Amaya, H., Kondo, K., and Hirata, H. 1998. Effect of chromium and molybdenum on corrosion resistance of super 13Cr martensitic stainless steel in CO₂ environment. *Corrosion/98*, Paper 113, NACE International, Houston, Tex.
5. Miyata, Y., Kimura, M., Toyooka, T., and Murase, F. Weldable martensitic stainless steel seamless pipe for linepipe application. Kawasaki report: 59-71.
6. Asahi, H., Hara, T., and Sugiyama, M. 1996. Corrosion performance of modified 13Cr OCTG. *Corrosion/96*, Paper 61, NACE International, Houston, Tex.
7. Pargeter, R. J., and Gooch, T. G. 1994. Welding for sour service. Update on sour service: materials, maintenance and inspection in the oil and gas industry. Conference, London: 17 pp.
8. Gooch, T. G. 1995. Heat treatment of welded 13%Cr-4%Ni martensitic stainless steel for sour service. *Welding Journal* 74(7): 213-s to 223-s.
9. Gooch, G. T., Woollin, P., and Haynes, A. G. 1999. Welding metallurgy of low carbon 13% chromium martensitic steels. *Proceedings of Supermartensitic Stainless Steels '99 Congress*, 188-195. Belgium.
10. Kimura, M., Miyata, Y., and Kitahaba, Y. 2001. Effect of retained austenite on corrosion performance for modified 13% Cr steel pipe. *Corrosion* 57(5): 433-439.

REPRINTS REPRINTS

To order custom reprints
of 100 or more of articles in
Welding Journal,
call FosteReprints at
(219) 879-8366 or
(800) 382-0808 or.
Request for quotes can be
faxed to (219) 874-2849.
You can e-mail
FosteReprints at
sales@fostereprints.com

Want to be a Welding Journal Advertiser?

For information, contact
Rob Saltzstein at
(800) 443-9353, ext. 243,
or via e-mail at
salty@aws.org.